Acta Biotheoretica
https://doi.org/10.1007/s10441-019-09351-1

REGULAR ARTICLE

On the Effect of Age-Dependent Mortality on the Stability of a System of Delay-Differential Equations Modeling Erythropoiesis

Frédéric Paquin-Lefebvre[1] · **Jacques Bélair**[2,3]

Received: 4 February 2019 / Accepted: 10 July 2019

Abstract
We present an age-structured model for erythropoiesis in which the mortality of mature cells is described empirically by a physiologically realistic probability distribution of survival times. Under some assumptions, the model can be transformed into a system of delay differential equations with both constant and distributed delays. The stability of the equilibrium of this system and possible Hopf bifurcations are described for a number of probability distributions. Physiological motivation and interpretation of our results are provided.

Keywords Erythropoiesis · Age-structured models · Delay-differential equations · Stability · Hopf bifurcation

1 Introduction

Haematopoiesis is the process by which stem cells differentiate and proliferate to supply the body with erythrocytes, platelets, neutrophils, macrophages, and many other specialized cells. These cells perform a number of body vital functions, and their production must therefore be carefully regulated. Changes in physiological conditions, such as the loss of blood due to a blood donation, a substantial hemorrhage, or lifestyle

✉ Jacques Bélair
belair@dms.umontreal.ca

Frédéric Paquin-Lefebvre
paquinl@math.ubc.ca

[1] Department of Mathematics, University of British Columbia, Vancouver, BC V6T 1Z2, Canada

[2] Département de mathématiques et de statistique and Centre de recherches mathématiques, Université de Montréal, CP 6128 Succ. centre-ville, Montréal, QC H3C 3J7, Canada

[3] Centre for Applied Mathematics in Bioscience and Medicine, McGill University, Montréal, Canada

Published online: 26 July 2019

changes such as excursion in high altitude or high intensity training, must be accounted for in the control of the cells.

Erythropoiesis, the production of red blood cells (RBCs), is a hierarchical process (Kaushansky et al. 2015; Wazewska-Csyzewska 1984): haematopoietic stem cells first differentiate into burst-forming units (BFU-Es), a self-sustaining population of cells responding to erythropoietin (Epo), the hormone that both stimulates reproduction of BFU-Es and causes further differentiation into colony-forming units (CFU-Es). From these, a series of cell divisions and proliferation produces proerythroblasts, basophilic erythroblasts, etc. until the stage of reticulocytes is reached, when cells then stop dividing and simply mature by increasing their hemoglobin content. Once reticulocytes have in turn matured enough, they lose their nuclei and then migrate to the blood stream from the bone marrow, where all previous steps take place. All stages of the maturation process are influenced by Epo, via a feedback mechanism rooted on monitoring of partial pressure of oxygen in the blood by a population of cells near the kidney.

Mathematical modeling of erythropoiesis has been an active area of research, significant efforts employing stage-structured models (Mahaffy et al. 1998), but other approaches having been used as well (Eymard et al. 2015 and references therein). In all cases, attention is given to the biological determination of the precise mechanisms of each of the steps in the production and control of erythrocytes: in particular, their maturation and aging, and the processes involved in the clearance of RBCs is of current interest (Arias 2017; Kaestener and Bogdanova 2014; Lang et al. 2012), as different mathematical formulations lead to different predictions regarding stability of equilibria (Bélair et al. 1995; Mahaffy et al. 1998). The work presented here follows this line of inquiries: we construct an age-structured model, simplifying the numerous erythropoietic steps by regrouping all cells into one of two compartments, which we label "precursor" and "mature". The aging process in each of the compartments, as well as the transition between compartments and the death of mature cells, is described phenomenologically using a framework more common in demography than physiology: cells are considered as "individuals".

Although it is common wisdom that RBCs live for about 120 days (Kaushansky et al. 2015), there is evidence that this lifespan is not exactly the same for all cells, but rather follows a distribution of ages (Shemin and Rittenberg 1946). Our motivation for the current formulation derives from a desire to understand the origin of this distribution, and attempt to pinpoint possible mechanisms influencing its properties.

2 Age-Structured Models for Haematopoiesis

We consider an age-structured population of erythrocytes that distinguish between precursor and mature cells. Let $p(t, \mu)$ and $m(t, \nu)$ be respectively the densities of precursor and mature cells, and let $\beta(\mu)$ and $\gamma(\nu)$ be respectively the birth rate of precursor cells and the death rate of mature cells. The aging process of all cells is then described by the following system of quasi-linear first-order hyperbolic partial differential equations (PDEs):

$$\frac{\partial p}{\partial t} + \frac{\partial p}{\partial \mu} = \beta(\mu)p, \quad t > 0, \quad 0 < \mu < \mu_F, \tag{2.1a}$$

$$\frac{\partial m}{\partial t} + \frac{\partial m}{\partial \nu} = -\gamma(\nu)m, \quad t > 0, \quad 0 < \nu < \infty, \tag{2.1b}$$

where μ_F is the maximal maturity level of precursor cells. Along with the system (2.1) two boundary conditions must be formulated to account for the recruitment of precursor cells from the undifferentiated stem cells and the transition from precursor to mature cells,

$$p(t, 0) = S_0(E(t)), \quad m(t, 0) = p(t, \mu_F), \tag{2.2}$$

where $E(t)$ is the time-dependent concentration of Epo, regulated by the total mature cell population through a negative feedback loop.

Following Bélair et al. (1995) and Mahaffy et al. (1998), we model the feedback function as a nonlinear Hill function defined by,

$$\mathcal{F}(M) = \frac{a}{1 + KM^r}, \quad M(t) = \int_0^\infty m(t, \nu)d\nu, \tag{2.3}$$

where $M(t)$ is the total population of mature cells. Now, if k is the per capita elimination rate of Epo, then an evolution equation for the hormone concentration is given by

$$\frac{dE(t)}{dt} = \mathcal{F}(M(t)) - kE(t). \tag{2.4}$$

Using the method of characteristics for first-order advection PDEs, we find that the large-time solution of the system (2.1) is given by

$$\begin{aligned} p(t, \mu) =& S_0(E(t - \mu)) \exp\left(\int_0^\mu \beta(\sigma)d\sigma \right), \\ m(t, \nu) =& p(t - \nu, \mu_F) \exp\left(- \int_0^\nu \gamma(\sigma)d\sigma \right). \end{aligned} \tag{2.5}$$

Following (Mahaffy et al. 1998), we suppose that the population of precursor cells grows exponentially until a certain threshold μ_1 is reached, giving the following proliferation rate,

$$\beta(\mu) = \begin{cases} \beta & \mu < \mu_1 \\ 0 & \mu \geq \mu_1 \end{cases}. \tag{2.6}$$

Such an assumption yields the following expression for the density of mature cells

$$m(t,\nu) = e^{\beta\mu_1} S_0(E(t-\nu-\mu_F)) \exp\left(-\int_0^\nu \gamma(\sigma)d\sigma\right). \tag{2.7}$$

We also suppose that the recruitment function $S_0(E)$ linearly increases with the level of hormone Epo.

Our goal is to investigate the effect of an age-dependent mortality rate $\gamma(\nu)$ on the stability of a population of erythrocytes at equilibrium. For this purpose, we let N be a random variable modeling the survival times of mature erythrocytes that follows a certain probability distribution with density function $f(\nu)$ and distribution function $F(\nu)$. The mortality rate, or hazard function, is defined as

$$\gamma(\nu) = \frac{f(\nu)}{l(\nu)} = -\frac{d}{d\nu}\log(l(\nu)), \tag{2.8}$$

where the quantity $l(\nu) = 1 - F(\nu)$ is the survival function, which is the probability of living longer than a certain age ν. Hence, given a certain mortality rate function $\gamma(\nu)$, it is possible to completely determine the associated survival times probability distribution, and expressions for the survival and probability density functions are obtained to be,

$$l(\nu) = \exp\left(-\int_0^\nu \gamma(s)ds\right), \quad f(\nu) = \gamma(\nu)\exp\left(-\int_0^\nu \gamma(s)ds\right), \tag{2.9}$$

from which we can readily establish that

$$\int_0^\infty f(\nu)d\nu = 1. \tag{2.10}$$

For the purpose of our study, we choose a mortality rate $\gamma(\nu)$ which increases exponentially as a function of the maturity level,

$$\gamma(\nu) = \theta e^{\theta(\nu-\nu_F)}, \quad \theta,\ \nu_F > 0. \tag{2.11}$$

Such a choice yields the following expressions for the survival function and the probability density function

$$l(\nu) = \exp\left(e^{-\theta\nu_F} - e^{\theta(\nu-\nu_F)}\right), \quad f(\nu) = \theta\exp\left(\theta(\nu-\nu_F) + e^{-\theta\nu_F} - e^{\theta(\nu-\nu_F)}\right). \tag{2.12}$$

We notice that the maturity level ν_F corresponds to the inflection point of the survival function, and thus to the maximal point of the probability density function. Finally, the expected value of the distribution E(N) is readily computed as,

$$\mathrm{E}(N) = \int_0^\infty l(\nu)d\nu = \frac{e^{e^{-\theta\nu_F}}}{\theta}E_1(e^{-\theta\nu_F}), \quad E_1(z) = \int_z^\infty \frac{e^{-\sigma}}{\sigma}d\sigma, \quad z > 0, \tag{2.13}$$

where $E_1(z)$ is the exponential integral function. Numerical quadrature is also required to compute the variance of the distribution $\mathrm{Var}(N)$, defined as

$$\mathrm{Var}(N) = 2\int_0^\infty \nu l(\nu)d\nu - \left[\int_0^\infty l(\nu)d\nu\right]^2. \tag{2.14}$$

The main properties of the distribution are plotted in Figs. 1, 2 and 3. We also remark that in the limit where the shape parameter θ approaches infinity, the distribution converges to a Dirac distribution centered in ν_F.

$$\lim_{\theta\to\infty}\gamma(\nu) = \lim_{\theta\to\infty}f(\nu) = \delta(\nu-\nu_F), \quad \lim_{\theta\to\infty}l(\nu) = \begin{cases} 1 & \nu \le \nu_F \\ 0 & \nu > \nu_F \end{cases} \tag{2.15}$$

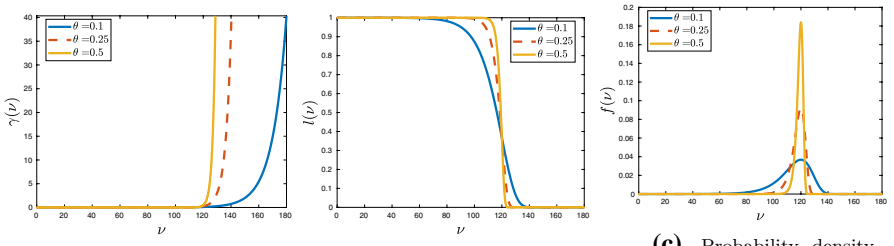

(a) Mortality rate function **(b)** Survival function **(c)** Probability density function

Fig. 1 Parameter values are $\nu_F = 120$ and $\theta = 0.1, 0.25, 0.5$

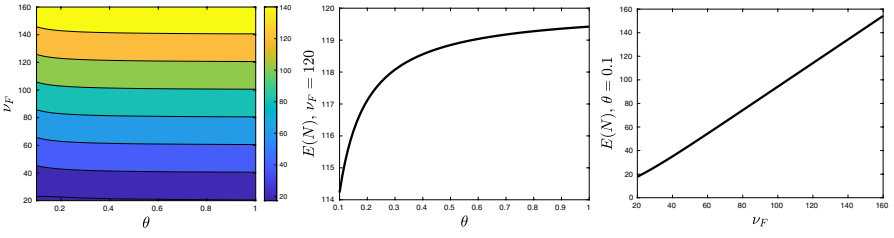

(a) Expected survival times. **(b)** $\nu_F = 120$ **(c)** $\theta = 0.1$

Fig. 2 Numerically computed expected survival times for different ν_F and θ values. In the middle panel, we notice that for a fixed $\nu_F = 120$, $\mathrm{E}(N)$ approaches ν_F as the shape parameter θ increases. The right panel shows a linearly positive correlation between $\mathrm{E}(N)$ and ν_F for a fixed $\theta = 0.1$

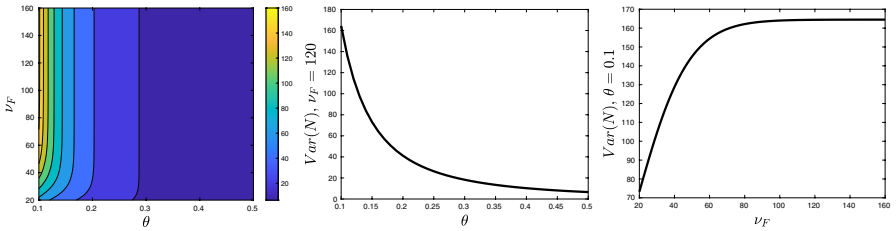

(a) Variance. **(b)** $\nu_F = 120$ **(c)** $\theta = 0.1$

Fig. 3 Numerically computed variance for different ν_F and θ values. The left and middle panels suggest $\mathrm{Var}(N)$ to be inversely proportional to the shape parameter θ. Conversely, for a fixed $\theta = 0.1$, the variance initially increases as a function of ν_F before reaching a plateau

3 System of Delay Differential Equations

Integrating Eq. (2.7) over all ages, we readily obtain an integro-differential system for the total population of mature cells and its regulatory hormone as

$$M(t) = \int_0^\infty e^{\beta\mu_1} S_0(E(t-\nu-\mu_F))l(\nu)d\nu, \tag{3.1a}$$

$$\frac{dE(t)}{dt} = \mathcal{F}(M(t)) - kE(t), \tag{3.1b}$$

which can be rewritten as a single equation for the regulatory hormone as,

$$\frac{dE(t)}{dt} = \mathcal{F}\left(\int_0^\infty e^{\beta\mu_1} S_0(E(t-\nu-\mu_F))l(\nu)d\nu\right) - kE(t). \tag{3.2}$$

Differentiating Eq. (3.1a) with respect to time and after integration by part, it is possible to obtain the following two-delay system:

$$\frac{dM(t)}{dt} = e^{\beta\mu_1} S_0(E(t-\mu_F)) - \int_0^\infty e^{\beta\mu_1} S_0(E(t-\nu-\mu_F))f(\nu)d\nu, \tag{3.3a}$$

$$\frac{dE(t)}{dt} = \mathcal{F}(M(t)) - kE(t), \tag{3.3b}$$

where the fixed delay corresponds to the age level at which precursor erythrocytes become mature, while the distributed delay accounts for the variable age of death of mature erythrocytes. In the limit where the survival times are all the same for each

erythrocyte, the distribution approaches a Dirac distribution and the second delay is simply reduced to a discrete delay as

$$\frac{dM(t)}{dt} = e^{\beta\mu_1}\big(S_0(E(t-\mu_F)) - S_0(E(t-\nu_F-\mu_F))\big), \tag{3.4a}$$

$$\frac{dE(t)}{dt} = \mathcal{F}(M(t)) - kE(t). \tag{3.4b}$$

3.1 Linear Stability Analysis

Let (M_e, E_e) be the total population and hormone level at equilibrium. After substitution into Eq. (3.3), we obtain that

$$E_e = \frac{\mathcal{F}(M_e)}{k}, \tag{3.5}$$

and thus for every $M_e > 0$, there exists a steady state solution of Eq. (3.3) for which the hormone concentration is given by (3.5). Such a translation invariance property of system (3.3) is a result of the time differentiation. Hence, from Eq. (3.1a) we readily establish that the total population of red blood cells at equilibrium satisfies

$$M_e = e^{\beta\mu_1} S_0'(E_e) E_e \int_0^\infty l(\nu)d\nu. \tag{3.6}$$

Next, we substitute (3.6) into (3.5) and obtain a single nonlinear algebraic equation for the steady state population,

$$\mathcal{F}(M_e) - \frac{kM_e}{e^{\beta\mu_1} S_0'(E_e)\int_0^\infty l(\nu)d\nu} = 0, \tag{3.7}$$

which possesses a unique solution $M_e > 0$ since the nonlinear Hill function is decreasing while $S_0'(E_e)$, the slope of the recruitment function, is strictly positive.

We can now proceed to a linear stability analysis by considering the following perturbation of the steady state solution,

$$\begin{pmatrix} M(t) \\ E(t) \end{pmatrix} = \begin{pmatrix} M_e \\ E_e \end{pmatrix} + \begin{pmatrix} \xi \\ \eta \end{pmatrix} e^{\lambda t}, \tag{3.8}$$

where $\lambda \in \mathbb{C}$ is the eigenvalue parameter while $(\xi, \eta)^T \in \mathbb{C}^2$ is the associated eigenvector. Inserting (3.8) into (3.3) and collecting coefficients of $e^{\lambda t}$ after linearization around the steady state yields the following linear homogeneous system

$$\begin{pmatrix} \lambda & -e^{\beta\mu_1} S_0'(\bar{E}) e^{-\lambda\mu_F}\left(1 - \int_0^\infty e^{-\lambda\nu} f(\nu)d\nu\right) \\ -\mathcal{F}'(\bar{M}) & \lambda + k \end{pmatrix} \begin{pmatrix} \xi \\ \eta \end{pmatrix} = \begin{pmatrix} 0 \\ 0 \end{pmatrix}. \tag{3.9}$$

For a non-trivial solution to exist, the system (3.9) must be singular and thus the eigenvalue parameter must satisfy a transcendental equation given by

$$\lambda(\lambda + k) + Ae^{-\lambda\mu_F}\left(1 - \hat{f}(\lambda)\right) = 0, \tag{3.10}$$

where $A = -e^{\beta\mu_1}S_0'(E_e)\mathcal{F}'(M_e) > 0$ is the gain in the nonlinear feedback loop between the total population of mature cells and the regulatory hormone Epo. We remark that $\hat{f}(\lambda) = \int_0^\infty e^{-\lambda\nu}f(\nu)d\nu$ in Eq. (3.10) is the Laplace transform of the probability density function $f(\nu)$.

We notice that since $\hat{f}(0) = 1$, Eq. (3.10) always possesses a root at the origin, which is a consequence of the translation invariance of steady state solutions. However, we can factor out the zero-eigenvalue simply by integrating by part the Laplace transform of the probability density function, which yields

$$g(\lambda) \equiv \lambda + k + Ae^{-\lambda\mu_F}\hat{l}(\lambda) = 0, \tag{3.11}$$

where $\hat{l}(\lambda)$ is the Laplace transform of the survival function. We also notice that the equation obtained in (3.11) exactly corresponds to the transcendental equation associated with the linearization of the integro-differential system (3.2).

Next, we consider the case for which the mortality rate function is given by (2.11) and investigate the loss of stability of the steady state. First, we readily notice that the only way this can happen is through a Hopf bifurcation, since substituting $\lambda = 0$ in (3.11) yields a negative gain in the feedback loop

$$A = -\frac{k}{\hat{l}(0)} < 0, \tag{3.12}$$

which is not possible. To determine the occurrence of a Hopf bifurcation, we substitute $\lambda = i\omega$ in (3.11) and upon separating the equation into real and imaginary parts, we obtain the following system:

$$k + A\left(\cos(\omega\mu_F)\int_0^\infty \cos(\omega\nu)l(\nu)d\nu - \sin(\omega\mu_F)\int_0^\infty \sin(\omega\nu)l(\nu)d\nu\right) = 0, \tag{3.13a}$$

$$\omega - A\left(\cos(\omega\mu_F)\int_0^\infty \sin(\omega\nu)l(\nu)d\nu + \sin(\omega\mu_F)\int_0^\infty \cos(\omega\nu)l(\nu)d\nu\right) = 0. \tag{3.13b}$$

Our goal is to investigate how the parameters A, ν_F and θ affect the stability of the equilibrium. Recall that ν_F corresponds to the maximal point of the probability density function $f(\nu)$, while the shape parameter θ controls the variance. Also, in the limit where $\theta \to \infty$, each mature erythrocyte dies at age ν_F and the distribution of survival times approaches a Dirac distribution. Upon computing the Laplace transform of the probability density function for such a limiting case, we obtain a simplified transcendental equation given by

Table 1 Two different sets of parameter values, taken from Bélair et al. (1995) and Mahaffy et al. (1998)

	Normal human	Rabbit with anemia
K	0.0382	0.0382
a (mU/ml/day)	6570	15600
r	6.96	6.96
k (day^{-1})	2.8	6.65
μ_F (days)	6	3
$M_e\left(\times 10^{11}\,\frac{\text{erythrocytes}}{\text{kg body mass}}\right)$	3.5	2.63

$$\lambda(\lambda + k) + Ae^{-\lambda\mu_F}\left(1 - e^{-\lambda\nu_F}\right) = 0. \tag{3.14}$$

For both cases where the survival times are distributed and constant, the nonlinearities inherent to the transcendental equation make it impossible to derive an explicit expression for the Hopf stability boundaries in the plane of parameters (ν_F, A). We use the software package COCO (Dankowicz and Schilder 2013) to compute a parameterization of those curves by the frequency ω.

Two different sets of parameters, corresponding to a normal human subject and to a rabbit with a certain periodic hematological disease, are considered here and given in Table 1. We keep ν_F and θ as bifurcation parameters, and mention that for a normal human the lifespan of mature erythrocytes is approximately 120 days, while for a rabbit it is approximately 50 days (Bélair et al. 1995; Mahaffy et al. 1998). Furthermore, we do not directly solve Eq. (3.7) for a population at equilibrium M_e since the slope of the recruitment function $e^{\beta\mu_1}S_0'(E_e)$ is unknown. Instead, given a certain population at equilibrium taken from Table 1, we can compute the slope as

$$e^{\beta\mu_1}S_0'(E_e) = \frac{kM_e}{\mathcal{F}(M_e)\int_0^\infty l(\nu)d\nu}. \tag{3.15}$$

Finally, we use this expression to parameterize a curve of equilibrium in a 2-D space of bifurcation parameters. That is, we can express the gain in the feedback loop as a function of ν_F (or θ),

$$A = -\frac{kM_e\mathcal{F}'(M_e)}{\mathcal{F}(M_e)\int_0^\infty l(\nu)d\nu}. \tag{3.16}$$

Hence, we have reduced the number of true bifurcation parameters to a single bifurcation parameter arising directly in the mortality rate function.

Several stability diagrams in the plane of the parameters ν_F and A are shown below. In Fig. 4 the fixed parameters correspond to a normal human subject, while in Fig. 5 they correspond to a rabbit with anemia. For each case, we investigate the effect of increasing the shape parameter θ and remark that the linear stability region shrinks as the distribution of survival times approaches a Dirac distribution. This once again shows that distributed delays, as opposed to their discrete analogs,

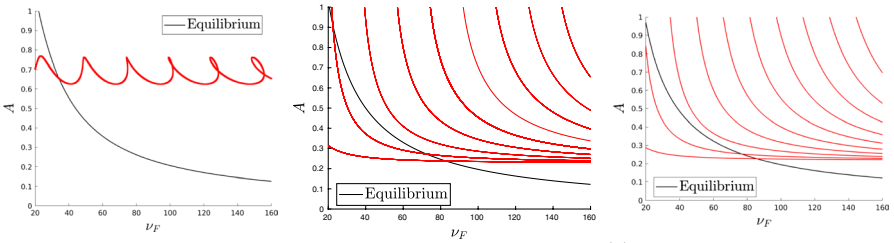

(a) $\theta = 0.1$ **(b)** $\theta = 0.5$ **(c)** Dirac distribution ($\theta \to \infty$).

Fig. 4 Hopf stability boundaries in the plane of parameters (ν_F, A) for three different values of θ. On each red curve, the linearization possesses purely imaginary eigenvalues. Other parameter values are $\mu_F = 6$ and $k = 2.8$, and are taken from the first column of Table 1. The equilibrium curve (black) is computed directly from (3.16) and the region of linear stability is located under the lowermost red curve. (Color figure online)

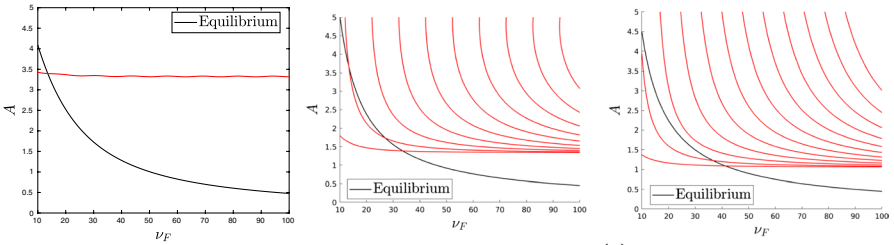

(a) $\theta = 0.1$ **(b)** $\theta = 0.5$ **(c)** Dirac distribution ($\theta \to \infty$).

Fig. 5 Hopf stability boundaries in the plane of parameters (ν_F, A) for three different values of θ. On each red curve the linearization possesses purely imaginary eigenvalues. Other parameter values are $\mu_F = 3$ and $k = 6.65$, and are taken from the second column of Table 1. The equilibrium curve (black) is computed directly from (3.16) and the region of linear stability is located under the lowermost red curve. (Color figure online)

enhance stability (Smith 2011). We also notice from Figs. 4 and 5 that the stability diagrams for $\theta = 0.5$ resemble closely the stability diagrams associated with the Dirac distribution. However, letting $\theta = 0.1$ yields qualitatively different diagrams containing a single curve, which can self-intersect for large ν_F values (see the first panel of Fig. 4). This indicates the presence of codimension-two double-Hopf bifurcation points, a typical instabilities of systems with multiple delays (Bélair and Campbell 1994; Stépán 1989). We expect the steady state to be unstable within each loop, since the purely imaginary eigenvalues will generically cross the imaginary axis, and thus, starting from the left-hand half-plane, will enter the right-hand half-plane. This has been numerically verified using the argument principle from complex analysis to count the number of roots of $g(\lambda) = 0$ in the right half-plane $\Re(\lambda) > 0$ (details not shown).

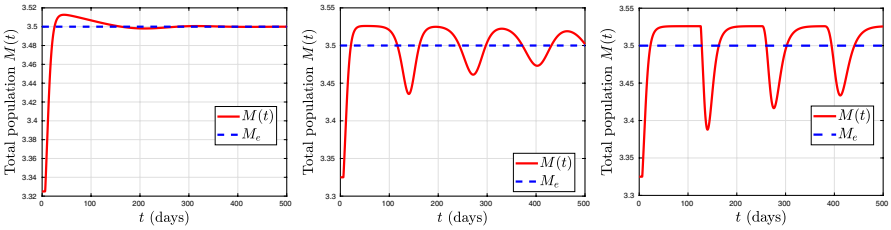

(a) $\nu_F = 120$, $\theta = 0.01$ **(b)** $\nu_F = 120$, $\theta = 0.1$ **(c)** $\nu_F = 120$, $\theta \to \infty$

Fig. 6 Return to equilibrium level following a blood donation in a normal human subject. Units are $\times 10^{11}$ erythrocytes per kg of body mass. The values of the other parameters are listed in the first column of Table 1

3.2 Numerical Simulations

In this section, we perform simulations to illustrate how the system behaves in the various parameter regimes identified in Figs. 4 and 5. Rather than solving the system of delay differential Eq. (3.3), for which the presence of a distributed delay makes it impossible to use any black-box DDE solver, we directly solve the integro-differential Eq. (3.2) employing a mixed collocation method (Brunner et al. 1997; Makroglou and Kuang 2006) that combines a classical implicit second-order Runge–Kutta scheme with trapezoidal integration. The details of this method are given in Appendix A. In the limiting case for which the model can be reduced to a system of delay differential equations having two discrete delays, we employ the DDE solver *dde23* from *Matlab*.

We first illustrate the role of the shape parameter θ on the stability of the equilibrium. More precisely, we address the problem of how quickly does the total population of erythrocytes return to its equilibrium level following a blood donation in a normal human subject. Such a numerical experiment has also been performed for the previous erythropoiesis models of Bélair et al. (1995) and Mahaffy et al. (1998). We fix $\nu_F = 120$ days and numerically solve the system for $\theta = 0.01, 0.1, \infty$, with initial and past conditions corresponding to 95% of the total population and hormone level at equilibrium. The results are shown in Fig. 6, where we conclude that the distribution of lifespans affects the strength of the oscillatory responses. As the shape parameter θ decreases, much more damped oscillatory responses are observed. In the Dirac distribution case, the discrete delays in the system cause a large population of erythrocytes to die exactly after 126 days: these are physiologically unrealistic, since blood banks allowing repeated blood donations every 56 days, normal levels are expected to be restored within this time period. We expect a normal individual to better regulate its population of erythrocytes, with the distribution of lifespans being a key mechanism behind homeostasis.

We then numerically investigate the onset of oscillations near a Hopf bifurcation as ν_F, the inflection point of the survival function, decreases. More precisely, the shape parameter is taken to be $\theta = 0.1$ with the other parameters taken from the

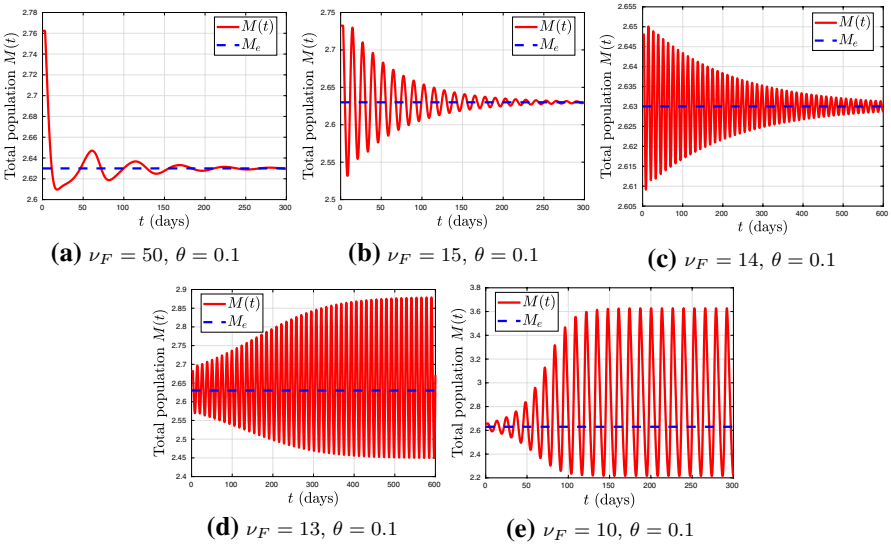

Fig. 7 Transition to sustained oscillations as ν_F decreases past a Hopf bifurcation. Other parameters are taken from the right column of Table 1. For each simulation, the initial and past conditions correspond to a random perturbation of the equilibrium levels. The predicted Hopf bifurcation point is $\nu_{F0} \approx 13.57$. In the last panel when $\nu_F = 10$ days and $\theta = 0.1$, the numerically computed oscillatory period is given by $T \approx 13.1$ days. This is close to the expected age of death, taking into account the 3 days required for precursor cells to reach the mature population

second column of Table 1. The Hopf bifurcation values predicted by the linear stability analysis are

$$\nu_{F0} \approx 13.5718,\ A_0 \approx 3.3963,\ \omega_0 \approx 0.51376, \tag{3.17}$$

where we recall that $\lambda_0 = \pm i\omega_0$ is the conjugate pair of purely imaginary eigenvalues at the bifurcation point. Moreover, the point in (3.17) exactly corresponds to the intersection point between the equilibrium curve (black) and the Hopf stability boundary (red) from the first panel of Fig. 5. It is beyond the scope of this study to determine the criticality of this Hopf bifurcation. We can nevertheless say that if the bifurcation were to be supercritical, then in the weakly nonlinear regime the system would branch off from the steady state to a stable limit cycle whose period is closely approximated by the linear period, here given by $T = 2\pi/\omega_0 \approx 12.2298$ days.

Numerical simulations for $\nu_F = 50$, 15, 14, 13, and 10 days are shown in Fig. 7, with these results suggesting a loss of stability through a supercritical Hopf bifurcation within the interval $13 < \nu_F < 14$. This example also illustrates the complexity of systems with multiple discrete and distributed delays. Here, the oscillations arise when ν_F decreases, which is somewhat contrary to the empirical fact in the delay differential equations community that small delays are harmless.

Finally, oscillations in the total population of various blood cells are typical of a class of diseases known as periodic hematological diseases (Foley and Mackey 2009). The example studied here suggests the origin of such pathological states to

be potentially linked to the average survival time of mature erythrocytes decreasing under some critical threshold.

4 Discussion

In this work, we have incorporated elements from survival analysis into an age-structured model for erythropoiesis. The novel aspect of this model is the survival times of mature erythrocytes that follow some physiologically realistic probability distribution for which the aging process increases the probability of death. This contrasts with previous modeling efforts which have supposed exponentially distributed (memoryless) survival times combined with some finite maximal lifespan (Bélair et al. 1995; Mahaffy et al. 1998).

We showed in Sect. 2 how a probability distribution can be recovered directly from the mortality rate function. In particular, the mortality rate studied here increases exponentially with the age level. The parameters determining this particular probability distribution consist of the inflection point of the survival function, which is a measure of the average lifespan, and of a shape parameter that controls the variance. Moreover, in the limit where the shape parameter is very large, the probability distribution approaches a Dirac distribution and each mature erythrocyte die at the same age level.

In Sect. 3, we first showed how the age-structured model can be ultimately reduced to either a single integro-differential equation for the regulatory hormone Epo, or to a system of delay differential equations having both a discrete and a distributed delays. We recall that the discrete delay accounts for the time required for the precursor cells to reach the mature population, while the distributed delay accounts for the variable age at which the mature erythrocytes die.

Linear stability analysis and numerical simulations are performed in the remainder of Sect. 3. In particular, we have addressed the loss of stability through Hopf bifurcations and the occurrence of sustained oscillations in the mature erythrocytes population. The bifurcation parameters considered here consist of the inflection point of the survival function ν_F, the shape parameter θ and the gain in the negative feedback loop A. For increasing values of θ, we have obtained a series of stability diagrams in the space of parameters defined by ν_F and A that emphasize the stabilizing effect of distributed over discrete delays. As expected, the region of linear stability shrinks as the shape parameter increases, corresponding to distributions that are highly concentrated around the average lifespan.

We first numerically investigated how quickly an erythropoietic system returns to its equilibrium level following a blood donation. Our results suggested that for a rapid return to equilibrium, the survival times must be widely distributed around the mean. We also numerically investigated the loss of stability through a Hopf bifurcation as the inflection point of the survival function (which is also a measure of the average lifespan) varies. Both the numerical simulations and the linear stability analysis suggested the oscillatory regime to be located below some critical threshold. From a physiological perspective, this experiment suggests that the early death of

mature erythrocytes could potentially be the origin of a class of pathological states known as periodic hematological diseases.

Finally, it would be interesting to analyze the model for other probability distributions that are widely used in survival analysis and demography. For example, a stochastic model for the survival times of red blood cells was developed in Korell et al. (2011), with a bathtub-shaped hazard function leading to an underlying modified Weibull probability distribution. In addition to the high mortality rate of old mature cells, such a distribution also takes into account early mortality potentially due to some physiological defects. Hence, it would be worthwhile to combine more sophisticated probability distributions with the modeling paradigm developed here.

Funding Partially supported by the Natural Sciences and Engineering Research Council of Canada (NSERC) as a Doctoral Scholarship to FPL and a Discovery Grant to JB.

Appendix A: Numerical Methods

In this section, we briefly describe the numerical methods behind the result of Sect. 3.2, which is adapted from Brunner et al. (1997) and Makroglou and Kuang (2006). Our goal is to compute a numerical solution to the following integro-differential equation

$$\frac{dE(t)}{dt} = \mathcal{F}(M(t)) - kE(t), \quad M(t) = \int_{-\infty}^{t} e^{\beta\mu_1} S_0(E(\sigma - \mu_F)) l(t-\sigma) d\sigma, \tag{A.1}$$

on some finite time interval $0 \le t \le t_f$ given any constant initial and past hormone level $E(t) = E_0$, with $t \le 0$. Now let us consider the equidistant mesh $t_j = jh$ with $j = 0, \dots, N$ and $h = t_f/N$, and let us furthermore suppose that the discrete maturation delay may be written as an integer multiple of the time-step as $\mu_F = Lh$, $L \in \mathbb{N}$. Applying a second-order Runge–Kutta scheme alongside with trapezoidal integration yields a system of $2N$ equations given by

$$\begin{aligned} M_j &= e^{\beta\mu_1} S_0(E_0) \int_{-\infty}^{0} l(t_j - \sigma) d\sigma + h \sum_{i=0}^{j} \alpha_i e^{\beta\mu_1} S_0(E_{i-L}) l(t_j - t_i), \\ E_j &= \frac{2}{2+hk} E_{j-1} + \frac{h}{2+hk} \left(\mathcal{F}(M_{j-1}) + \mathcal{F}(M_j) - kE_{j-1} \right), \end{aligned} \tag{A.2}$$

for the unknowns (M_j, E_j), $j = 1, \dots, N$. We remark that in Eq. (A.2), $E_{i-L} = E_0$ if $i \le L$ while the α_i are the usual weights for trapezoidal quadrature defined by,

$$\alpha_i = \begin{cases} \frac{1}{2} & i = 0 \text{ or } N, \\ 1 & 0 < i < N. \end{cases} \tag{A.3}$$

Fortunately, the presence of the discrete maturation delay makes it possible to explicitly solve the system A.2 given any constant initial and past hormone level E_0.

References

Arias CF (2017) How do red blood cells know when to die? R Soc Open Sci 4:160850
Bélair J, Campbell SA (1994) Stability and bifurcations of equilibria in a multiple-delayed differential equation. SIAM J Appl Math 54(5):1402–1424
Bélair J, Mackey MC, Mahaffy JM (1995) Age-structured and two delay models for erythropoiesis. Math Biosci 128:317–326
Brunner H, Makroglou A, Miller RK (1997) Mixed interpolation collocation methods for first and second order Volterra integro-differential equations with periodic solution. Appl Numer Math 23(4):381–402
Dankowicz H, Schilder F (2013) Recipes for continuation. In: Computational science & engineering, vol 11. Society for Industrial and Applied Mathematics (SIAM), Philadelphia
Eymard N, Bessonov N, Gandrillon O, Koury M, Volpert V (2015) The role of spatial organization of cells in erythropoiesis. J Math Biol 70:71–97
Foley C, Mackey MC (2009) Dynamic hematological disease: a review. J Math Biol 58(1–2):285–322
Kaestener L, Bogdanova A (2014) Regulation of red cell life-span, erythopoiesis, senescence, and clearance. Front Physiol 5:269. https://doi.org/10.3389/fphys.2014.00269
Kaushansky K, Lichtman M, Prchal J, Levi MM, Press OW (2015) Williams hematology 9E. McGrawHill, New York
Korell J, Coulter CV, Duffull SB (2011) A statistical model for red blood cell survival. J Theor Biol 268:39–49
Lang E, Qadri SM, Lang F (2012) Killing me softly—suicidal erythrocyte death. Int J Biochem Cell Biol 44:1236–1243
Mahaffy JM, Bélair J, Mackey MC (1998) Hematopoietic model with moving boundary condition and state dependent delay: application in erythropoiesis. J Theor Biol 190:135–146
Makroglou A, Kuang Y (2006) Some analytical and numerical results for a nonlinear volterra integro-differential equation with periodic solution modeling hematopoiesis. Hellen Eur Res Math Inf Sci 9:21–37
Shemin D, Rittenberg D (1946) The lifespan of the human red blood cell. J Biol Chem 166:627–636
Smith H (2011) An introduction to delay differential equations with applications to the life sciences. Texts in applied mathematics, vol 57. Springer, New York
Stépán G (1989) Retarded dynamical systems: stability and characteristic functions, vol 210. Pitman Research Notes in Mathematics Series. Longman Scientific & Technical, Harlow
Wazewska-Csyzewska M (1984) Erythrokinetics—radioisotopic methods of investigation and mathematical approach. US Department of Commerce National Technical Information Service